Mechanisms Leading to Co-existence of Gas and Hydrate in Ocean Sediments

Technology Status Assessment

for

U.S. Department of Energy
National Energy Technology Laboratory
DOE Award DE-FC26-06NT43067

by

Ruben Juanes
Department of Civil and Environmental Engineering
Massachusetts Institute of Technology
77 Massachusetts Avenue, Room 48-319
Cambridge, MA 02139
Phone: 617-253-7191, Fax: 617-258-8850
Email: juanes@mit.edu

Steven L. Bryant
Department of Petroleum and Geosystems Engineering
The University of Texas at Austin
One University Station, Mail Stop C0300
Austin, TX 78712
Phone: 512-471-3250, Fax: 512-4719605
Email: Steven_Bryant@mail.utexas.edu

November 30, 2006

TABLE OF CONTENTS

List of Figures

List of Acronyms

BSR	Bottom Simulating Reflector
DEM	Discrete Element Method
HSZ	Hydrate Stability Zone
IODP	Integrated Ocean Drilling Program
LSM	Level Set Method
ODP	Ocean Drilling Program
PFC	Particle Flow Code (commercial trademark)

1 CURRENT STATE OF TECHNOLOGY

1.1 Summary of Background of Industry/Sector

1.1.1 Introduction

Methane hydrates are crystalline ice-like compounds, composed of methane molecules caged in a lattice of water molecules [Sloan, 1998]. Hydrates form naturally at high pressures and low temperatures, like those typical of most of the ocean floor (**Figure 1**).

It is believed that an enormous pool of carbon exists in the form of methane gas and methane hydrate in the ocean floor along the continental margins [Kvenvolden, 1988; Kvenvolden et al., 1993; Judd et al., 2002]. Some estimates of the size of this reservoir [Holder et al., 1984; Collett, 2002; Ruppel, 2006] suggest that the amount of energy is equivalent to twice that of all other fossil fuels combined [Sloan, 2003]. Even if these estimates are in great error, this energy resource deserves careful examination [Milkov, 2004]. It also seems likely that this pool of carbon –largely ignored until recently– plays an important role in the global carbon cycle [Dickens, 2003]. Dissociation of methane hydrates in the ocean floor has also been linked to massive submarine landslides [Paull et al., 1996, 2003] and global warming [Dickens, 1999; Judd et al., 2002].

The widely accepted conceptual model for the presence of methane hydrates in ocean sediments can be briefly summarized as follows: methane of biogenic or thermogenic origin is generated in deep oceanic sediments, where the temperature is high enough for the methane to be a gas. Methane bubbles grow and link, eventually having sufficient buoyancy for upwards migration. In the shallow sediments, however, where the temperature is much colder, the methane gas will lead to the formation of hydrates. This defines the Hydrate Stability Zone (HSZ), whose thickness depends on the depth of the ocean floor (**Figure 2**).

There are still many open questions related to occurrence and distribution of hydrates in the ocean floor, and it is probably fair to say that the knowledge of these systems as a whole is in a stage of infancy. We divide our exposition of the state-or-the-art into the following sections:

1. Occurrence and distribution in natural systems
2. Laboratory experiments of hydrate-bearing sediments
3. Micromechanical theories of hydrates in porous media
4. Macroscopic modeling of natural hydrate systems

1.1.2 Occurrence and Distribution in Natural Systems

Methane hydrate systems in ocean sediments have been the subject of intense research in recent years. A significant component of that effort is directed towards gaining a better conceptual picture of the hydrogeological environment of gas hydrate systems. Particular attention has been devoted to the two end-members [Trehu et al., 2006b]:

1. The hydrogeologically more active, dynamic end-member, exemplified by Hydrate Ridge, offshore Oregon (see, e.g. [Suess et al., 1999; Tryon et al., 2002; Trehu et al., 2004b]). This

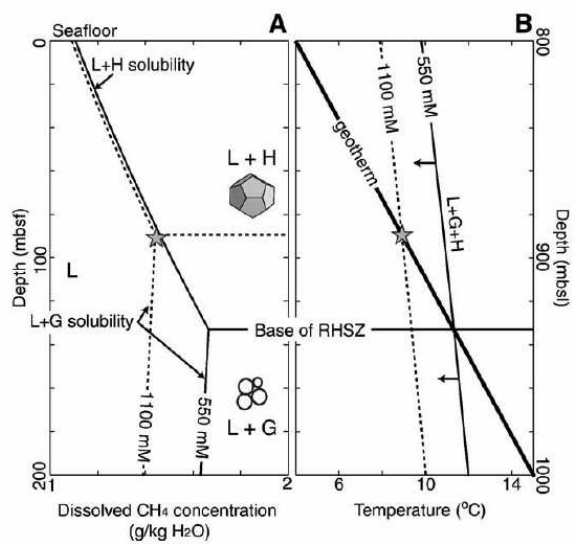

Figure 1: Diagram illustrating **(a)** methane solubility, **(b)** temperature for three-phase (hydrate–gas–brine) equilibrium as a function of depth for two salinities. The diagrams assume that water depth is 800 m, a seafloor temperature of 4°C, a hydrostatic pressure gradient of 10 MPa/km, and a geothermal gradient of 5.5°C/km. Methane hydrate (H) and methane gas (G) exist only if the methane concentration exceeds solubility. The peak in solubility determines the bottom end of the hydrate stability zone (HSZ). Since methane solubility decreases with water salinity, the bottom of the HSZ is shallower for higher chlorine content. [Liu and Flemmings, 2006].

system displays focused flow through fractures, episodic releases of methane gas and highly variable methane gas and methane hydrate distributions. Other aspects related to the dynamic nature of Hydrate Ridge have been discussed in the literature, including the importance of lateral flow [Weinberger et al., 2005], and inference of gas venting sites with gas bubbles with a hydrate shell [Heeschen et al., 2003].

2. The hydrogeologically less active, quiescent end-member, illustrated by Blake Ridge, offshore South Carolina [Holbrook et al., 1996; Dickens et al., 1997].

One of the fundamental observations at these two sites is the co-existence of methane hydrate, gas and brine within the HSZ. This is especially noticeable in dynamic environments [Milkov et al., 2004b; Torres et al., 2004], but has been observed in low-flux hydrate provinces [Gorman et al., 2002]. There is by now conclusive evidence that methane transport through the HSZ cannot occur solely as dissolved methane in the aqueous phase. The scientific community is now undergoing a heated debate as to what are the reasons for co-existence [Milkov and Xu, 2005; Torres et al., 2005; Ruppel et al., 2005], which include: (1) kinetics of hydrate formation; (2) regional geotherms; (3) hypersaline brines as a result of hydrate formation; and (4) fast, focused flow of free gas through fractures and high-permeability conduits. The importance of methane migration as a separate gas phase, and the need to account for multiphase flow effects coupled with hydrate formation, have already been pointed out a decade ago [Ginsburg and Soloviev, 1997; Soloviev and Ginsburg, 1997].

It has been proposed that free gas accumulation beneath the HSZ may reach a critical thickness to open fractures in the sediment or activate pre-existing faults that will serve as conduits for fast upwards gas migration [Flemings et al., 2003; Trehu et al., 2004a; Hornbach et al., 2004; Liu and Flemmings, 2006; Weinberger and Brown, 2006]. In this case, it is clear that the study of the hydrate system must be coupled with the mechanical response of the host sediments containing hydrate.

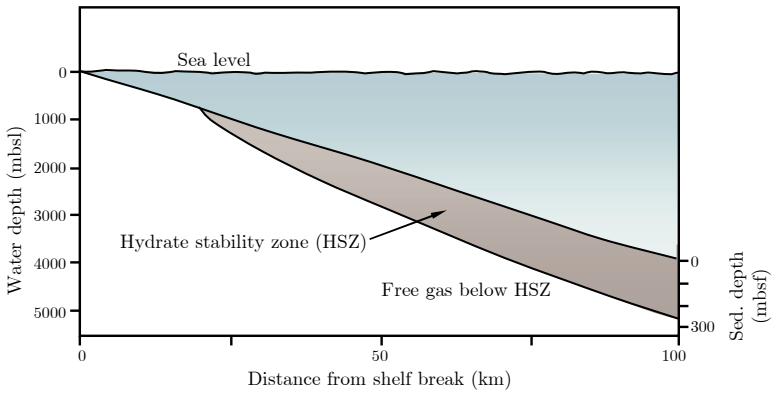

Figure 2: Idealized cross section of the hydrate stability zone (HSZ) along a continental shelf. The thickness of the HSZ increases with the depth of the sea floor. After Dickens [2003].

1.1.3 Laboratory Experiments of Hydrate-bearing Sediments

In recent years, the scientific community has undertaken a number of laboratory investigations to elucidate key aspects of the behavior of gas hydrates in porous materials. Here, we restrict our attention to two related topics: (1) hydrate nucleation and growth, and (2) mechanical response of the hydrate-bearing sediment.

There continues to be controversy as to where the hydrate forms within the porous medium [Waite et al., 2004]. Dvorkin et al. [2000] considered four pore-scale hydrate distributions, with the following two end-members: (1) hydrate floating in the pore fluid; (2) hydrate cementing at the grain contacts. Clearly, the two scenarios behave would very differently in terms of acoustic and mechanical properties of the composite medium [Ecker et al., 1998; Guerin et al., 1999; Tinivella and Accaino, 2000; Kleinberg et al., 2003; Yun et al., 2005]. A number of investigations has addressed this issue, but the results are equivocal. Some differences may be attributed to the guest molecule employed (e.g. methane, CO_2 or tetrahydrofuran) although the hydrate formation method is probably at least as important as the hydrate former itself [Lee et al., 2006]. Gas percolation experiments indicate that methane forms around the grain contacts, and then grows inwards into the pore space [Waite et al., 2004; Winters et al., 2004]. The reason is that hydrate forms at the gas–water interface, which for low water saturations will be near the grain contacts due to preferential wetting to water. This was confirmed by visualization experiments in glass micromodels [Tohidi et al., 2001]. On the other hand, experiments in which the guest molecule is dissolved in water show that hydrate forms preferentially in the pore space, without cementing the solid skeleton [Tohidi et al., 2001; Yun et al., 2005, 2006].

Several research groups have recently launched extensive laboratory investigations for the determination of mechanical properties of hydrate-bearing soils and sediments at large strains [Yun et al., 2006; Durham et al., 2005; Ebinuma et al., 2005; Masui et al., 2005]. Recent investigation illustrates that bubble growth in soft marine sediments leads to highly eccentric oblate spheroids (disks), suggesting that the medium responds as fracturing elastic solid [Johnson et al., 2002; Boudreau et al., 2005], in contrast to the fluid-like plastic response typical of soft (cohesion-less) sands [Wheeler, 1988; Sills et al., 1991].

1.1.4 Micromechanical Theories of Hydrates in Porous Media

At the pore scale, a conceptual model of hydrate formation in marine sediments was proposed by Clennell et al. [1999] and Henry et al. [1999]. This capillary-thermodynamic model can explain some observations concerning hydrate distribution in relation to pore size and sediment type. It cannot explain by itself, however, the heterogeneity at all scales that is observed in natural marine sediments [Trehu et al., 2006b].

In addition to thermodynamic arguments, the kinetics of hydrate formation play a major role in both laboratory experiments and geologic scenarios. For example, Genov et al. [2004] visualize gas hydrates grown at gas–ice interfaces, and provide a mechanistic model of hydrate growth that includes: (1) hydrate film spreading, (2) clathration, and (3) diffusive gas and water transport through the hydrate shell. Such kinetic processes keep the hydrate–gas–sediment system away from equilibrium, and may retard (or inhibit) hydrate formation during the flow of methane gas through the HSZ [Zatsepina and Buffett, 2003].

1.1.5 Macroscopic Modeling of Natural Hydrate Systems

Several continuum models have been developed for the mathematical modeling of methane transport within the HSZ. Rempel and Buffett [1997] derive an one-dimensional analytical model assuming dissolved methane and equilibrium between hydrate and seawater. They find that the model cannot explain the volumes of hydrates observed, and they extend it in a heuristic way to incorporate transport of methane gas. Davie and Buffett [2001] propose a one-dimensional mathematical model that accounts for sedimentation, organic degradation and variable salinity, with which they could explain observed behavior at Blake Ridge [Davie and Buffett, 2003]. In the (steady-state) Darcy-type model of Xu and Ruppel [1999], the flow of methane gas is accounted for explicitly. They conclude that diffusion of methane within the aqueous phase alone is insufficient to explain hydrate accumulations observed in natural systems, and therefore advection must be an essential transport mechanism. Nimblett and Ruppel [2003] derive a one-dimensional transient model to incorporate changes in permeability due to hydrate precipitation, but free methane gas is ignored. Torres et al. [2004] proposed a one-dimensional transient model with variable pore-water salinity. They concluded that measured chlorinity data in Hydrate Ridge can only be explained if methane is transported in its own gas phase.

At the field scale, numerical simulation of hydrate-bearing systems is currently being pursued, most notably by the Lawrence Berkeley National Lab [Moridis, 2003; Moridis et al., 2004, 2005]. Their numerical simulation model accounts for four-phase nonisothermal flow, and includes both an equilibrium and kinetic model for hydrate formation and dissociation. Much of the emphasis of these investigations is on production enhancement by thermal and chemical stimulation, while paying less attention to the hysteresis effects associated with multiphase flow [Kumar et al., 2005; Juanes et al., 2006], and coupling with sediment mechanics. In a project funded under this DOE/NETL program, however, a team of investigators from Texas A&M, UC Berkeley and Lawrence Berkeley National Lab plan to extend these numerical simulation capabilities by incorporating the mechanical effects explicitly [Holditch et al., 2006].

1.2 Technologies, Tools, Approaches and Data Being Used

An excellent review of current technologies for the exploration and characterization of hydrate-bearing ocean sediments is given in Trehu et al. [2006b]. They organize the technologies and tools in two groups: (1) remote sensing, and (2) ocean drilling.

1.2.1 Remote Sensing

The primary tool for the exploration of methane hydrates in ocean sediments is *seismic studies.* These geophysical investigations permit detection of a Bottom Simulating Reflector (BSR) associated with the bottom of the hydrate zone [Stoll et al., 1971]. While the presence of a BSR indicates that gas hydrates are present, the amount of hydrate and underlying free gas cannot be easily inferred. On one hand, the seismic velocity depends strongly on the microscale distribution of hydrate [Ecker et al., 1998; Helgerud et al., 1999; Guerin et al., 1999; Yun et al., 2005]. On the other, hydrates can occur without a BSR due to co-existence of gas and hydrate in the HSZ.

Other techniques are currently being investigated for detection and quantification of methane hydrates and methane gas, including *electromagnetic sounding* [Weitemeyer et al., 2005], *ocean-bottom seismology* [Hobro et al., 2005; Backus et al., 2006], *seafloor compliance* [Willoughby et al., 2005] and *sidescan reflectivity* [Roberts et al., 2006].

1.2.2 Ocean Drilling

Drilling into the ocean floor has provided the most direct evidence of the presence and distribution of hydrate in marine sediments [Trehu et al., 2006b]. The Ocean Drilling Program (ODP) and its successor, the Integrated Ocean Drilling Program (IODP) have been instrumental for advancing our knowledge of hydrates in ocean sediments. Recent expeditions have concentrated on two major hydrate provinces: Blake Ridge (ODP Leg 164 [Paull et al., 2000] and Hydrate Ridge (ODP Leg 204 [Trehu et al., 2006a], IODP Expedition 311 [Riedel et al., 2006]). Also very recently, the DOE/Chevron Joint Industry Project has undertaken ocean drilling in hydrate-bearing sediments in the Gulf of Mexico [Claypool et al., 2006].

Conventional coring does not preserve in situ pressure during retrieval of the core sample. As a result, hydrate typically dissociates and the analysis must rely on geochemical proxies such as total gas volume, pore water chloride concentration, or methane–ethane ratio [Milkov et al., 2004a]. Pressurized coring was introduced in ODP Leg 164 [Dickens et al., 1997] and used in other expeditions Milkov et al. [2003]. The technology for pressure cores has advanced tremendously in the past few years, and now permits analysis of many physical properties at in situ conditions (see Box 8.1 in Trehu et al. [2006b] and the references therein).

Infra-red cameras are based on the principle that hydrate dissociation is endothermic, and produces temperature anomalies. These "cold spots" can be quickly and systematically scanned by infra-red cameras to identify hydrate-bearing intervals and estimate gas distribution [Weinberger et al., 2005].

Other useful techniques for inferring the presence of hydrate and constraining its amount are downhole geophysical logs (logging-while-drilling [Riedel et al., 2006]), vertical seismic profiles [Trehu et al., 2006a], and in situ temperature measurements [Ruppel, 2000; Riedel et al., 2006].

1.3 Benefits and Inadequacies of Current State-of-the-Art

The main benefit of the current state-of-the-art is the volume of data. A decade of intense research has produced direct observations of methane hydrate accumulations in ocean sediments in sufficient number to illustrate the complexity of hydrate growth habits and of gas and hydrate distributions within the hydrate stability zone. The main inadequacy is theoretical: the state of the art in modeling teaches that it is not straightforward to explain the observed complexity of hydrate distribution. Our knowledge has improved dramatically over the past few years, yet many questions remain. Thus the field is poised to take advantage of mechanistic models that can predictively and quantitatively describe hydrate growth and distribution. Such models can be tested against available measurements with enough rigor to permit useful inferences about what mechanisms must be relevant in the hydrate stability zone, and what mechanisms are unlikely to play a role. These inferences will guide further model development and more crucially can suggest key experiments or measurements that would help resolve competing explanations.

The above remarks motivate the focus of this project on mechanistic modeling, as described in the next section. Here we note that state-of-the-art models of hydrate distribution at the continuum scale do not yet account for several essential features of the natural system. These features include:

- a three-dimensional spatial description;
- true multiphase flow;
- relative permeability and capillary pressure data, including the hysteresis between gas-advancing and water-advancing behavior;
- the mechanics of the sediment, including the effect of pore pressure and multiple fluid phases in the pore space.

The importance of the interface between gas and water phases in the growth habit of hydrates demands that it be carefully treated at the relevant length scales, especially at the grain-scale. Here the historical difficulty has been the geometric description of the grain space (or, equivalently, the pore space) in real sediments, or in realistic models of such sediments. When capillary forces are important, as in this application, the computational challenge (finding surfaces of constant curvature) is also significant. Recent advances in high-resolution X-ray imaging of sediments and in lattice-Boltzmann models for fluid flow are promising. However, it would be very difficult to extend these approaches to account for an essential characteristic of methane hydrate accumulations, namely the substantial spatial dislocation of sediment grains that accompanies fracturing of the sediment. In contrast, the simpler approaches to determining fluid configurations that will be used in this project are readily integrated with grain-scale mechanics models.

2 DEVELOPMENT STRATEGIES

2.1 Why New Approach is Required?

Significant gaps remain in our knowledge of the behavior of hydrate systems in marine sediments. In relation with the scope of the proposed project, we highlight the following:

1. Until now, relatively simple models have been developed for the quantitative prediction of methane distribution within the HSZ [Rempel and Buffett, 1997; Davie and Buffett, 2001; Xu and Ruppel, 1999; Nimblett and Ruppel, 2003; Torres et al., 2004; Liu and Flemmings, 2006].

2. Particularly urgent is the need to account rigorously for the simultaneous flow of methane gas and brine. In fact, the need for heterogeneous models that include multiphase flow has been highlighted in several investigations [Soloviev and Ginsburg, 1997; Trehu et al., 2004b; Milkov and Xu, 2005; Torres et al., 2005]

3. To date, little or no attention has been paid to hysteresis that takes place naturally when fluid displacements are in response to episodic events (drainage and imbibition cycles).

4. More realistic models are required to incorporate the effect of hydrate formation on fluid flow properties (permeability impairment) [Torres et al., 2004]

5. Transport models must be coupled with sediment mechanics (fracture initiation and propagation) and must consider the multidimensional effects of lateral methane migration (along beds) in the prediction of vertical, buoyancy driven flow.

6. Ultimately, many scientific questions remain. What are the causes for co-existence of three phases in the HSZ: kinetics of hydrate formation, water availability, capillary suppression, hypersaline pore waters? Which cause dominates? What are the impacts on the size and producibility of the methane reservoir in marine sediments?

The key observation is that a great deal of the observed behavior of hydrate accumulations in natural geologic systems depends on the local (grain-scale) geometry of the gas–water interface. Some of the relevant factors include:

1. Gas distribution: movement, filtration and distribution of the gas phase through the porous medium as driven by capillary pressure.

2. Mass transfer: (1) of methane and water through the hydrate film; (2) of ions from the brine side of the hydrate skin towards the bulk aqueous phase.

3. Mechanical strength: (1) additional cohesion forces resisting fracture initiation; (2) additional resistance to capillary invasion.

4. Heat transfer: latent heat of freezing from the hydrate skin to the surroundings.

5. Seismic properties: wave speed and attenuation.

We propose to model methane transport and hydrate formation in ocean sediments at the grain scale and at the bed scale. The bed scale model will incorporate insights (characteristic length or time scales, average macroscopic behavior, etc.) from the grain scale models. The latter include models of sediment structure, of capillarity-controlled interfaces in sediments, and of sediment mechanics. The models are mechanistic and have been used successfully in many geologic applications. We will couple these models and use them to explore whether gas-phase methane transport tends to be self-limiting or self-reinforcing. The premise that hydrate forms at a gas/water interface has implications for the distribution and growth habit of hydrate. The explicit models of gas/water interface geometry at grain- and bed-scales allow us to examine the implications of this premise quantitatively. We will compare the characteristic behaviors of the models with field observations reported in the literature.

The proposed solution is model- and simulation-based. We know well the potential pitfalls for simulation-based research, and adopt this approach for two reasons. First, a continuum theory that accounts for the grain scale processes important in this application has not yet been developed. Quantitative work thus requires computer simulation. Second, the proposed grain-scale computations are on physically realistic domains and do not invoke adjustable parameters. The results therefore afford physical insight and can be tested against experimental observations. They can even motivate new experiments. This capability is particularly useful when experiments are difficult or expensive, as is the case with methane hydrates in sediments.

In the next section we describe the proposed approach in two parts. First we present our conceptual model of hydrate-bearing ocean sediments. Then we outline the coupling, integration and application of existing models, and the development of new models.

2.2 Problems to be Addressed in this Research Project

2.2.1 Conceptual Model

The conceptual picture illustrated and described in **Figure 3** highlights the phenomena of interest in this proposal. The single most important ingredient of our conceptual model is the simultaneous flow of water and methane gas during the formation of methane hydrate within the HSZ. This premise is firmly grounded on field observations (see, e.g. Tryon et al. [2002]; Milkov et al. [2004b]; Torres et al. [2004])

Several phenomena must play a role in any sediment in which hydrate is forming as a result of gas and brine phases coming into contact. One phenomenon is capillarity. The geometry of an interface between two fluid phases in a sediment is controlled by capillary forces. The interface is not a single uninterrupted entity; at the grain scale it occupies many individual pore throats simultaneously. Because methane and water movement are often driven by episodic forcing events, capillary hysteresis is inevitable (**Figure 4**). Consequently, the distribution of fluid phases within sediment, and hence the distribution of hydrate, will be a complicated function of the forcing events and the grain-scale structure of the sediments.

A second key process is undersaturated sediment mechanics, that is, the mechanical behavior of the sediment in the presence of several fluid and solid phases in the pore space (water, gas and hydrate). While capillarity governs invasion of gas through the porous medium, mechanical effects

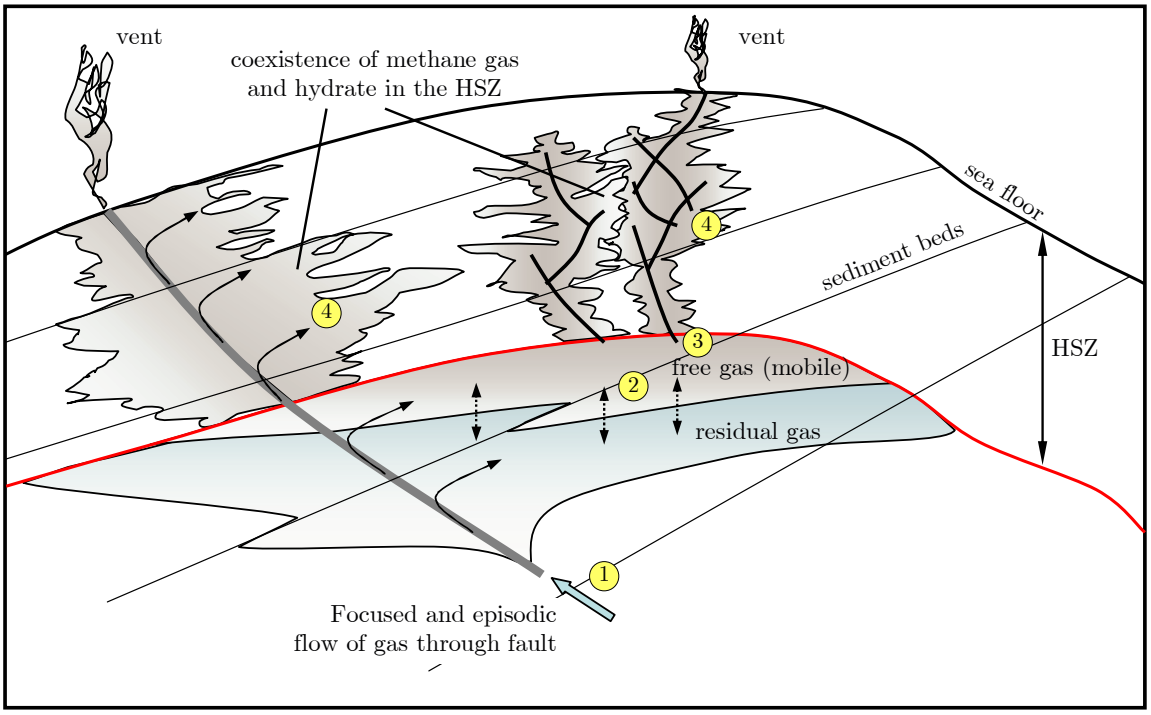

Figure 3: Conceptual model of methane hydrates in ocean sediments proposed in this research. The model involves the following key physical processes: (1) Focused and possibly episodic upwards flow of gas through faults, fractures and high-permeability conduits; (2) Presence of a laterally-extended free mobile gas zone beneath the HSZ, whose height responds to gradual build-up from deep methane gas and episodic release into the HSZ; (3) Vertical invasion of methane gas from below the HSZ, either by exceeding the capillary entry pressure or the fracturing pressure; (4) Lateral invasion of methane gas into sediment beds, also by the two modes of invasion [Remark: the thresholds for capillary pressure and fracture opening invasion are dependent upon pre-existing hydrate in the pore space]; (5) Increase in pore-water salinity by ion exclusion from the hydrate crystalline structure – ion diffusion out of macroscopic drainage areas can be very slow; [Remark: processes 5-7 occur at the grain scale and are not explicitly depicted] (6) Imbibition events (water saturation increases locally) that are driven by the inability to maintain gas pressure due to the finite volume of free gas beneath the HSZ – imbibition leads to capillary trapping and a complex distribution of methane gas and methane hydrate; (7) Possible rupture of hydrate shell around disconnected volumes of gas, responsible for increased mobility of methane and formation of additional gas–water interface.

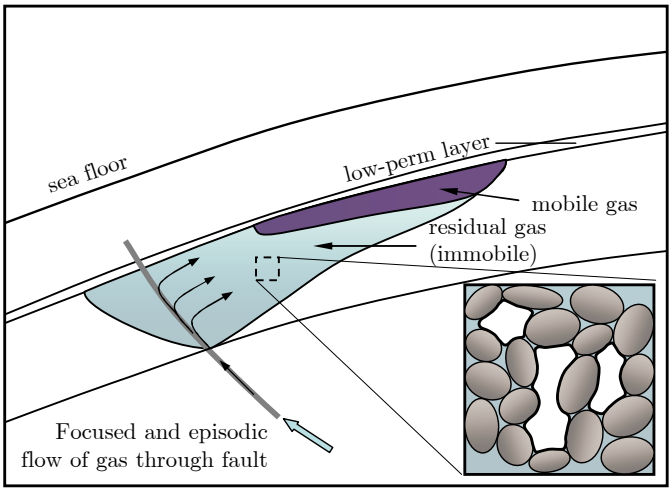

Figure 4: Residual (immobile) gas saturation results from capillary trapping during an imbibition process (increasing water saturation). Trapping can occur below and within the HSZ, a consequence of the irreversible character of multiphase displacement in porous media: capillary pressure and relative permeability functions exhibit hysteresis. Imbibition takes place naturally during the upwards migration of methane through the sediment whenever the methane is driven by episodic events in which the pressure is not held constant.

may lead to deformation and fracturing of the sediment skeleton, thereby triggering invasion when it would otherwise not occur (**Figure 5**). Methane invasion by fracture opening is common, as evidenced by field observations of tensile fractures at the seafloor and hydrate layers along bedding planes (**Figure 6**). The fracturing pressure in this application is exerted by a gas phase. The gas pressure acts upon the non-wetted surfaces of the sediment grains. Moreover, the water held at grain contacts as pendular rings increases the cohesion of the sediment [Orr et al., 1975; Lian et al., 1993; Willett et al., 2000], which in turn affects the mechanical response (**Figure 7**). These processes clearly couple flow and deformation, at both the grain scale and the macroscopic scale.

A third phenomenon is buoyancy-driven flow. Methane rising within a sediment, either through a fracture formed by the methane or as a drainage displacement front, can establish a vertically continuous column of gas. The capillary pressure at the top of the gas column increases as the column height increases. On one hand this increases the ability of the gas phase to continue to propagate. On the other, it also increases the probability that the rising gas will overcome capillary entry pressures and drain laterally into sediment beds, thereby weakening fracture propagation. This coupling raises the important possibility of self-limiting and self-reinforcing modes of propagation (**Figure 8**). Determining the geologic conditions under which each mode occurs is one goal of this research.

Taken together, these three phenomena already exhibit a rich variety of behavior. Understanding this behavior is a necessary but not sufficient condition for understanding the growth habit of hydrates in ocean sediments. Clearly the precipitation of hydrates at gas/water interfaces will increase the resistance to methane movement whether by drainage or by fracture propagation and will alter the mechanical properties of the sediments. On the other hand, hydrate occupies considerably less volume than its stoichiometric components under typical ocean sediment conditions. Thus the pressure within a disconnected volume of gas will decrease as hydrate forms, raising the possibility of breaking or dislodging the rigid hydrate barrier (**Figure 9**). Dissolved salts are excluded from the hydrate lattice, so the remaining water becomes more saline, decreasing hydrate stability. These effects will be amplified in sediments because a drainage displacement produces a highly ramified gas phase geometry, (**Figure 10**), with a large ratio of interface area to water volume. Depending

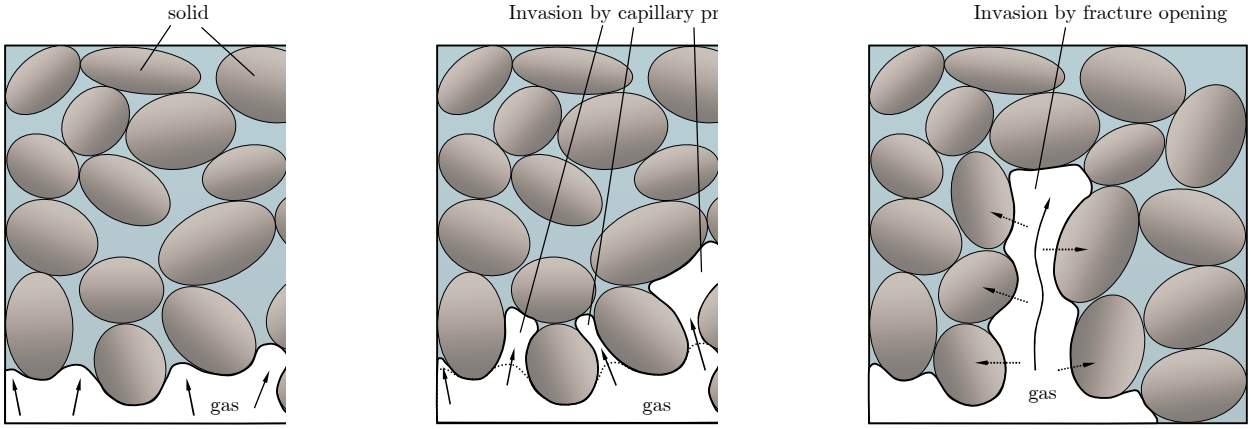

Figure 5: Schematic diagram of the two modes of methane gas invading a sediment. **Left:** before invasion, the gas–water interface of a buoyant gas plume underlies water-filled sediment. **Center:** invasion will occur if the capillary pressure (the difference between gas pressure and water pressure) exceeds the capillary entry pressure, which is inversely proportional to the pore diameter. **Right:** invasion by fracture opening; if the exerted pressure is sufficient to overcome compression and friction at grain contacts, a fracture will form. In a multiphase environment, due to surface tension effects, the gas pressure will *not* dissipate quickly through the porous medium, and water at grain contacts will increase cohesion.

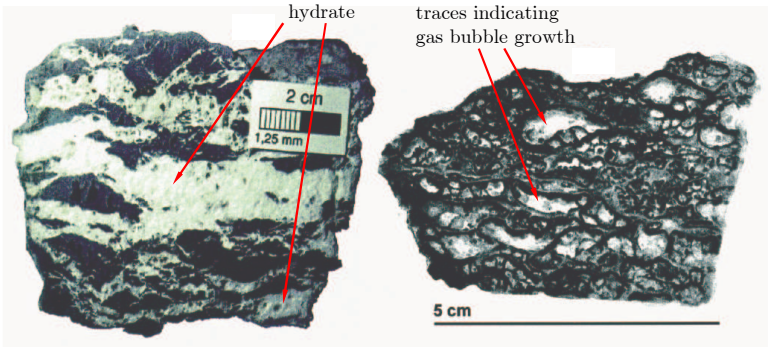

Figure 6: Hydrate fabric in ocean sediments. **Left:** The figure shows hydrates occurring in discrete layers that are several millimeters or centimeters thick, generally parallel to bedding; the hydrate does not occupy the original pore space but, rather, has opened a fracture. **Right:** internal structure of the hydrate shows traces of gas bubbles, indicating that it is likely that hydrate precipitation was organized around the gas–water interface. [Suess et al., 1999]

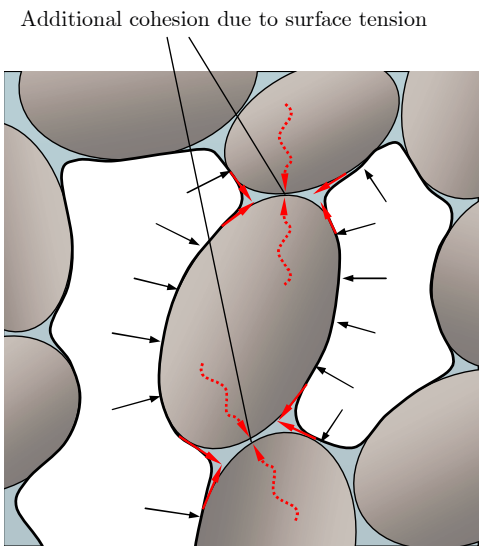

Figure 7: Meniscus pinning in the presence of two fluid phases in the sediment. During multiphase flow in porous media, the least wetting phase (gas) migrates through the center of the pores, while the most wetting phase (brine) coats the grains and forms filaments around the crevices of the pore space. This configuration leads to gas–water menisci around the grain contacts. Due to interfacial tension, these menisci are responsible for an attraction force between grains. At the macroscopic level, this can be interpreted as an increment in the cohesion of the material. This is a purely multiphase-flow effect, not present in single-phase poromechanics.

on the capillary pressure, much of the water phase within the drained sediment may be connected only by surface films on sediment grains. Thus the interaction between hydrate formation, capillarity and sediment mechanics could lead to hydrate distributions that differ qualitatively from those governed by a subset of these processes.

2.2.2 Development and Integration of Models

Models of granular media. Phenomena at the grain scale – capillarity, sediment fracturing, hydrate formation at gas/water interfaces – are fundamental to this application. We propose to study the interactions of these phenomena in a class of simple granular materials: dense random packings of spheres. The radius distribution of the spheres can be chosen to reflect different types of sediment. Random packings of spheres are remarkably powerful models for understanding sediments, even though real grains are rough, angular, non-spherical objects. This is because several key features of void space depend fundamentally upon the random arrangement of the grains rather than their shapes (**Figure 11**).

Random packings of equal spheres were proposed as "ideal soils" a century ago [Morrow and Graves, 1970; Slichter, 1899], and early studies [Hackett and Strettan, 1928; Haines, 1927, 1925] yielded insights into the limiting values of capillary pressure for drainage and imbibition, the hysteretic nature of drainage and imbibition, and the role of pendular rings of wetting phase at grain contacts. But quantitative work is not possible without knowledge of the locations of the grains. Thus theoretical attention turned to regular packings [Graton and Fraser, 1935; Pirson, 1947; Bradley, 1980] until Finney [1970] measured the locations of more than 8000 grains in a dense, random packing of ball bearings. Mason soon used those measurements to extract the frequency distribution of pore throat sizes in Finney's packing, from which he estimated capillary pressure curves (phase volume fraction vs applied capillary pressure) in unconsolidated granular material [Mason, 1972]. Mason and Mellor [1995] subsequently introduced a network model that explicitly

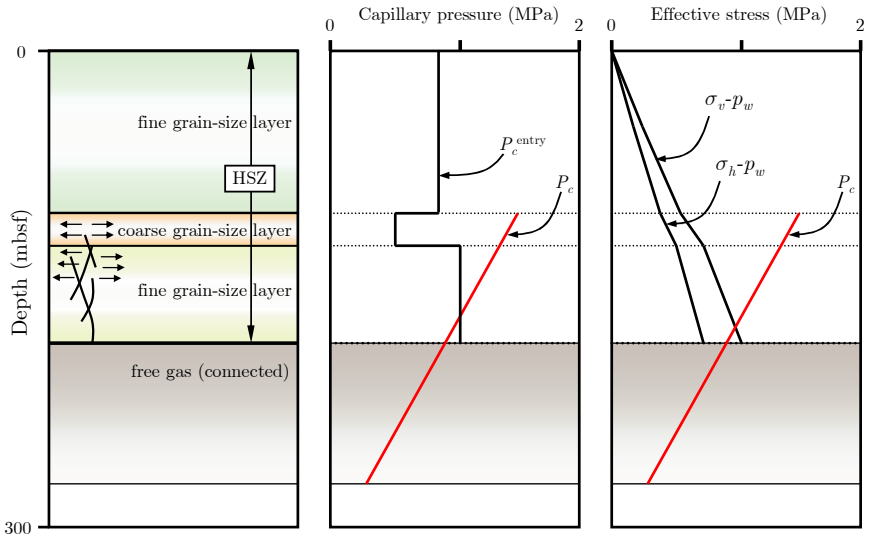

Figure 8: Conceptual profiles of capillary entry pressure and minimum principal stress vs sediment depth. **Left:** A connected, mobile, free gas zone exists underneath the HSZ. Gas will migrate upwards if the capillary pressure is sufficient to overcome the capillary entry pressure or if the gas pressure is sufficient to fracture the sediment. **Center:** The capillary entry pressure P_c^{entry} is higher in fine-grain sediments, because it is inversely proportional to the pore diameter. If the gas phase is connected, the capillary pressure P_c increases with elevation. The situation depicted is such that $P_c < P_c^{\text{entry}}$ at the bottom of the HSZ, so gas cannot invade. However, if gas were to invade by opening a vertical fracture (right panel), the capillary pressure would exceed P_c^{entry} at higher elevations, leading to lateral invasion of sediment beds *above* the bottom of the HSZ. **Right:** The vertical (lithostatic) stress increases with depth in excess of hydrostatic stress. In this figure we plot the difference between the stress and pore water pressure for both vertical and horizontal stresses. If the capillary pressure exceeds the minimum horizontal stress, a vertical fracture will propagate, serving as a conduit for upwards gas migration. This is the case depicted here. These fractures will open in response to episodic releases of methane and can transport methane gas to shallower beds, from which gas may flow laterally by capillary or fracture invasion.

accounted for the spatial locations of pore throats and their connectivity within the Finney packing. Numerically generated packings [Torquato, 2002] can also be used. For this project we will use a version of the cooperative rearrangement algorithm that produces geologically reasonable model sediments [Thane, 2006].

Knowledge of grain locations also permits calculation of transport properties. Roberts and Schwartz [1985] used Finney's data to calculate electrical conductivity in packings of nonconducting grains filled with a conducting fluid. The PI adapted the approach of Mason and Mellor [1995] to predict hydraulic conductivity in sandstones [Bryant et al., 1993]. Starting with the original Finney packing, the void fraction was varied by increasing the radius of the spheres, without changing the sphere locations. The characteristic length scale is set by the known diameter of the original grains of sand; all other information is derived from the known locations of the spheres in the Finney pack. Thus the predictions of hydraulic conductivity, which agree with the observed trend over a range of five orders of magnitude, contain no adjustable parameters. Though the model is clearly an oversimplification of naturally occurring materials, evidently it captures the features of the void space in such material that control single-phase fluid flow. This is confirmed by independent

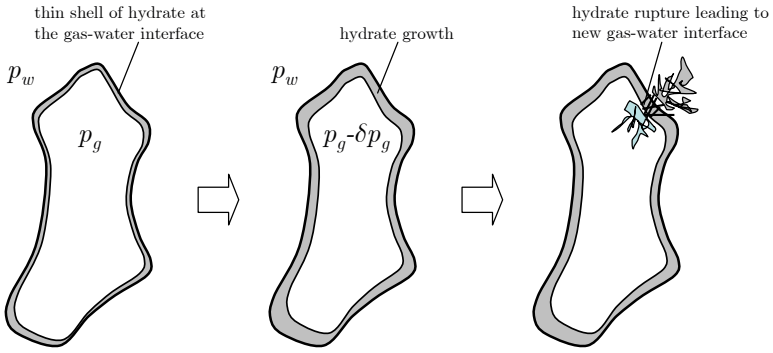

Figure 9: Hydrate precipitates as a thin layer around the gas–water interface. The volume occupied by hydrate is less than that of its stoichiometric components. Thus if the hydrate layer is rigid, the pressure inside the volume of gas will decrease, eventually leading to mechanical instability and rupture of the hydrate shell. This is a potential mechanism for enhancing the mobility of methane gas and providing additional gas–water interface area.

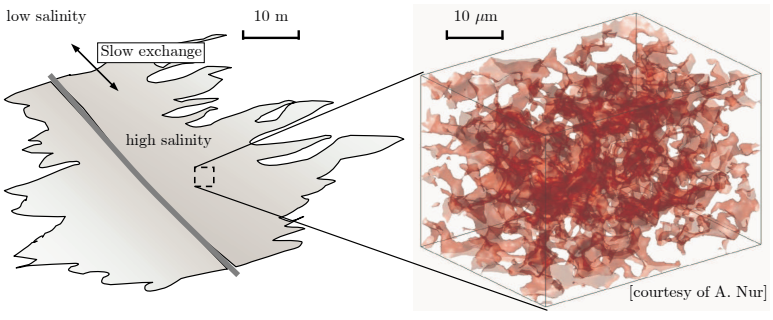

Figure 10: Pore-water salinity increases locally during hydrate formation because ions are excluded from the hydrate lattice. If the chlorine concentration is sufficiently high, hydrates will no longer form (**Figure 1**). Drainage creates a large gas-water interfacial area in contact with small volumes of water (right figure). Thus hydrate formation can be understood as an equilibrium reaction locally. Restoring seawater salinity within the drained region would requires ion diffusion over macroscopic distances (left figure), a very slow process. The increase in salinity in the invaded sediment is therefore likely to be pervasive and may hinder hydrate formation significantly.

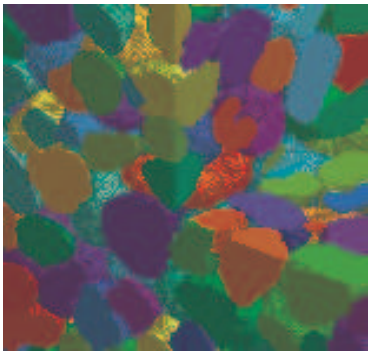

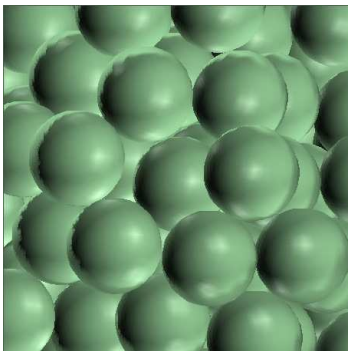

Figure 11: We use dense random packings of spheres as model sediments. **Left:** CT image of naturally occurring granular material (sandstone), courtesy K. Thompson of LSU. The colors are selected by a novel post-processing algorithm that distinguishes individual grains. **Right:** A model sediment (Finney's random packing of equal spheres). The model sediment is disordered, and this simple feature captures many important aspects of the pore-scale geometry of a real sediment.

predictions of drainage, imbibition and fluid/fluid interfacial area [Bryant et al., 1996; Gladkikh and Bryant, 2005, 2003; Bryant and Johnson, 2004].

With the advent of high resolution 3D imaging of real rocks and sediments [Jin et al., 2003; Lindquist et al., 2000; Blunt and Hilpert, 2001; Arns et al., 2003; Willson et al., 2004; Fredrich and Lindquist, 1997], sphere packs may appear quaint. They are appropriate for this project, however, because the objective is to understand the behavior of the coupled physical phenomena, rather than to understand a particular sediment or hydrate deposit. As illustrated below, the methods to be used are not limited to spheres. If it turns out that some aspects of the behavior depend crucially upon grain shapes, for example, then it will be straightforward to study that case with the methods developed in this project. Our experience indicates that remarkably simple models capture key features of real sediments and thus are a useful starting point.

Representing pore space in granular media. Inspection of granular materials, (**Figure 11**), reveals two essential features: the sizes of the constrictions in the void space vary widely, and the voids are interconnected in a complicated way. The network model [Fatt, 1956] –a graph of sites (pores) connected by bonds (pore throats)– captures both features when geometric attributes are assigned to sites and bonds. Consequently the network model has been widely used for relating macroscopic transport properties to pore-level geometry, and the literature is vast (cf. review in Blunt and Hilpert [2001] and Reeves and Celia [1996]; Rajaram et al. [1997]). The key difference between our approach and many previous ones is that our networks are extracted directly from the model sediment. We note that it is possible to compute transport properties in the actual pore space without invoking a network. When two fluids occupy the pore space, however, networks prove to be quite convenient.

Several methods exist for mapping the void space of a porous medium onto a network, including medial axis analysis [Lindquist et al., 2000], Voronoi tessellation [Roberts and Schwartz, 1985], and Delaunay tessellation [Mason and Mellor, 1995]. The latter is convenient for studying fluid configurations in packings of spheres. Applied to the coordinates of the sphere centers, Delaunay tessellation defines groups of nearest neighbor spheres. Each set of nearest neighbors contains four spheres whose centers define a tetrahedron, (**Figure 12**). The void space in this tetrahedron corresponds naturally to a pore body, while the void area in each face corresponds naturally to a pore throat.

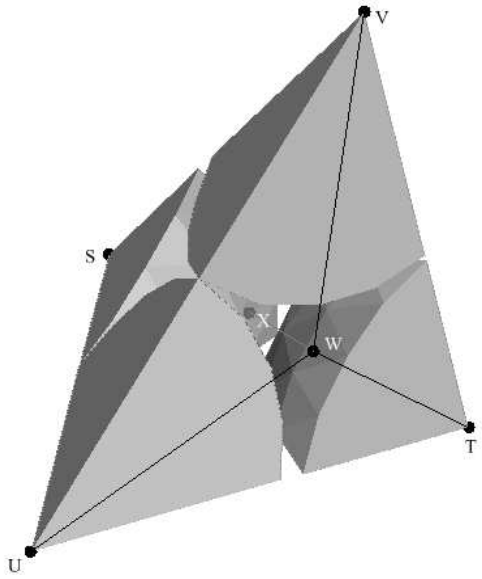

Figure 12: Delaunay cell from a dense random sphere packing defines pore bodies (cell interior, centered at X) and throats (void area in cell faces, centered at W) directly from the known locations of the sphere centers.

The network representation of void space associates each Delaunay cell with a site. Each pair of sites corresponding to adjacent cells is connected with a bond. The geometric attributes of the network elements, e.g. the diameter of a pore throat, are determined directly from the geometry of the corresponding tetrahedron. Thus the network obtained from Delaunay tessellation replicates the topology and geometry of the void space in the sphere packing. Consequently, properties that depend on pore-scale geometry can be computed *a priori*.

Computing capillarity-controlled displacement. The classical network representation of fluid configurations consists of labels for each site and each bond that identify the fluid phase occupying that network element. The labels define complementary sub-networks, and macroscopic properties specific to one fluid are calculated in the appropriate sub-network. The task at hand is to determine the set of labels when surface tension controls the pore-level configuration. For typical applications we must also account for history: which fluid initially occupies pore space, how capillary pressure was changed to effect displacement, etc.

Several methods are available. Invasion percolation [Wilkinson and Willemsen, 1983] is ideally suited to the quasi-static displacement process implied by surface tension control. The idea is that the displacing fluid "invades" the pore space one throat (or one pore) at a time in response to small increments (decrements) in capillary pressure. Capillary pressure is assumed to be global, existing wherever a fluid/fluid interface is found. A necessary condition for an invasion event is that the applied capillary pressure be greater (less) than the critical pressure for the corresponding throat (pore). The value of critical pressure depends strongly on the geometry of the throat (pore). To determine the critical pressure, we use level set methods, as described in next section.

Level set methods and capillarity-controlled interfaces. A level set method tracks the evolution of an interface [Sethian, 1999; Osher and Feldkiw, 2002; Osher and Sethian, 1988]. The

interface is embedded as the zero level set of a function $\phi(x,t)$ which evolves according to

$$\phi_t + F|\nabla\phi| = 0, \qquad \phi(x, t=0) \quad \text{given.} \tag{1}$$

We have implemented this method with speed function F given by

$$F(x,t) = a \exp\left[f\left(1 - \frac{V(t)}{V_m}\right)\right] - b\kappa(x,t) \tag{2}$$

The first term is pressure-like with a prescribed pressure a, target volume V_m and bulk-modulus f. $V(t)$ is the non-wetting phase volume, b is the surface tension term, and $\kappa(x,t)$ is the mean curvature of the interface. The steady state solution of Eq. (2) is a constant curvature solution. We account for the porous medium by imposing a constraint of the type $\phi(x,t) \leq \psi(x)$ where ψ is a fixed level set function that describes the pore space.

We use a progressive quasi-static algorithm to find the critical pressure for a given pore throat or body. Starting from an arbitrary initial interface location, we increment (for drainage; decrement for imbibition) the pressure by Δa and evolve Eq. (1) to steady state. Far from the critical pressure, the location of the zero level set at the new steady state is close to the former location. At the critical pressure, the increment (decrement) causes the interface to jump to a new pore body or throat.

We illustrate this approach in simple 2D pore space [Prodanovic and Bryant, 2006a]. In the drainage simulation (**Figure 13**) the algorithm correctly identifies that the left-most throat has the smallest critical pressure. In the imbibition simulation (**Figure 14**), the algorithm correctly identifies the critical configuration as the point at which the meniscus moving down through the upper throat touches the meniscus moving to the left through the right hand throat. We remark that this simulation independently confirms the applicability of the Melrose criterion [Melrose, 1965] for a pore-level imbibition event. Gladkikh and Bryant [2005] have shown that this criterion leads to correct predictions of macroscopic behavior unique to imbibition displacements, and gives a mechanistic explanation for hysteresis.

We have already implemented this approach in three dimensions [Prodanovic and Bryant, 2006b] and will use it for this project.

Discrete Element Modeling of pore-scale mechanics. The Discrete Element Method (DEM) [Cundall and Strack, 1979] has proved a valuable tool to study the mechanisms for deformation and failure of granular materials with variable degree of cementation [Bruno and Nelson, 1991]. Moreover, based on simple geometric arguments, stress variations (and subsequent deformation) have been shown to affect flow properties such as porosity and permeability [Bruno, 1994].

Each element or grain is identified separately by its own mass, moment of inertia and contact properties. For each grain, its translational and rotational movements are described by solving Newton's second law of motion. The mechanical behavior at the deformation region of grain contact is approximated by introducing a grain contact model, such as a system of a spring, dashpot and slider (**Figure 15**). The movement of a grain is dictated by the net force and moment acting on it. For a *dry model*, that is, one in which pore pressures are negligible, the forces for each grain may include: (1) contact force $\boldsymbol{F}_c$ due to the deformation at the grain contacts, (2) damping forces $\boldsymbol{F}_d$

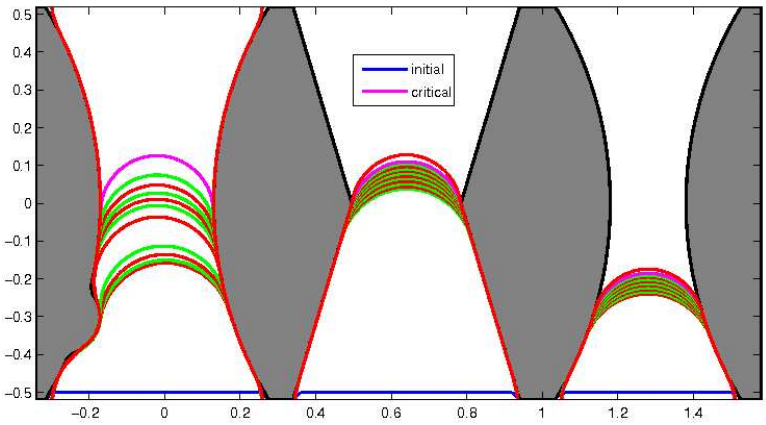

Figure 13: A complete sequence of the progressive quasi-static algorithm for drainage in three throats in parallel. The dark gray areas are solid grains. Colored curves are the zero level sets corresponding to the wetting/nonwetting meniscus at a series of pressures. Initial interface position is shown in blue at bottom of diagram, and the subsequent steps alternate in red and green colors. The critical pressure step is in magenta color. The method correctly identifies that the leftmost throat drains first. The menisci remain in the middle and right throats at that curvature.

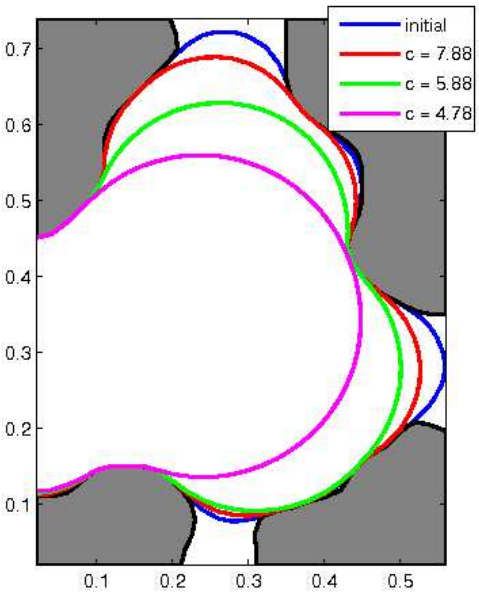

Figure 14: Imbibition simulation in a 2D pore, cut from a slice of a segmented 3D X-ray microtomography image. Color conventions as (**Figure 13**). Imbibition started from a drainage endpoint with three menisci (blue curves). As capillary pressure decreases, the menisci in bottom and right-hand throats merge (green). When the merged meniscus touches the meniscus in the top throat (magenta), the pore imbibes.

due to grain non-elastic collisions; (3) external forces $\boldsymbol{F}_b$ due to gravity and prescribed tractions at the boundaries. The contact force $\boldsymbol{F}_c$ can be further split into normal and tangential components, $\boldsymbol{F}_c^n$ and $\boldsymbol{F}_c^t$, respectively.

Bulk behavior of a granular system is determined by all individual grain–grain interactions. For the analysis of *dry samples*, that is, systems in which the pore pressure is negligible, the interactions between particles can be associated with a network of grain–grain contact forces that connects the *centroids* of grains that are in contact (**Figure 16**).

The motion of an individual grain in the multi-grain system is determined by the resultant force $\boldsymbol{F}$ and moment $\boldsymbol{M}$ acting upon it. The grain motion can be described by the following

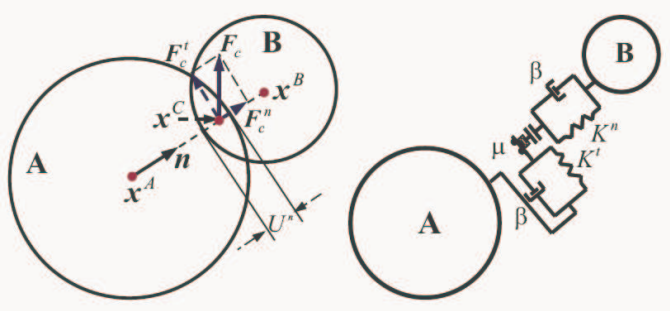

Figure 15: Schematic diagram of a grain–grain contact (left) and the associated contact model in a Discrete Element Model (right) [Jin, 2006].

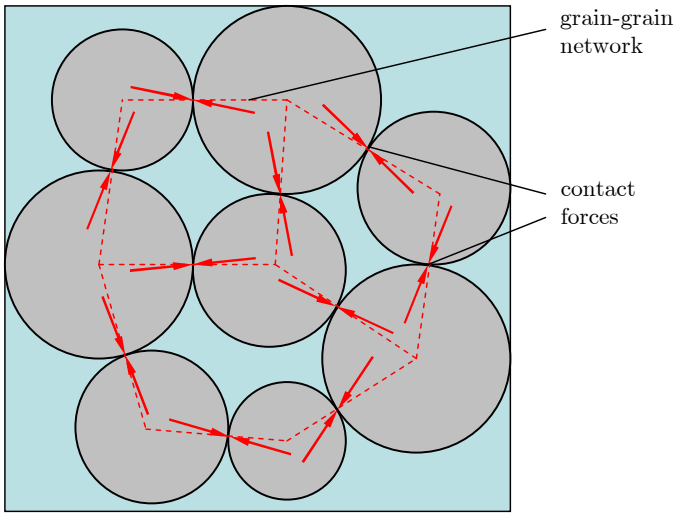

Figure 16: Schematic diagram of the network of grain–grain contact forces. Even though the contact forces generally involve a normal and tangential component, their action can be associated with a network that connects the centers of grains that are in contact. This network of forces is sufficient to characterize "dry samples".

equations of motion:

$$m\ddot{\boldsymbol{x}} = \boldsymbol{F}, \tag{3}$$

$$I\ddot{\boldsymbol{\theta}} = \boldsymbol{M}. \tag{4}$$

Here, $\boldsymbol{x}$ and $\boldsymbol{\theta}$ are the position vector of the grain centroid and the angle vector of rotation about the centroid; the double dots denote second time derivatives of the position and rotation angle; and m and I are the mass and moment of inertia, respectively. The equations of motion (3)–(4) must be solved simultaneously for all grains in the system via a numerical integration scheme. In DEM, explicit solution schemes with a single force evaluation per time step are preferred. A commercial three-dimensional DEM code, PFC3D [ITASCA, 2005], will be used.

Coupling multiphase fluid displacement and mechanics in Discrete Element Models. Most DEM applications are restricted to dry samples, and do not consider the influence of the pore pressure on the mechanical equations. From the theory of poromechanics [Biot, 1941], it is well known that pore pressure will influence mechanical behavior. Essentially, compressive stresses in granular media are transmitted both through a solid skeleton and the pore fluids. Recently, models have been developed to incorporate this effect in Discrete Element Models *with a single-phase pore fluid* [Shimizu, 2004; Cook et al., 2004]. Other models have been developed for incorporating the effect of wetting pendular rings [Muguruma et al., 2000; Yang et al., 2003]. These models, however, make hard assumptions at the time of placing the wetting phase in the pore space: an even distribution of liquid volume among gaps smaller than the rupture distance.

Here, we are interested in a quasi-static description of fluid displacement, and its impact on the mechanical behavior. With reference to **Figure 7**, the presence of a two-fluid system in the pore space will lead to two new types of forces in a DEM model:

1. *Pore fluid forces* caused by the pressure exerted by the fluid occupying the center of pore bodies.

2. *Capillary forces* due to menisci present in pore gaps. These forces lead to adhesion and, as a result, incremental cohesion and mechanical strength of the granular medium.

In **Figure 17** we illustrate how to incorporate these sets of forces. Pore-fluid forces belong to a network that links pore bodies with its nearest grain centers (obtained from a Delaunay tesselation of the sediment model). The force is computed through an appropriate integration of the pore pressure. It is important to note that this pressure may be the water pressure or the gas pressure, depending on pore occupancy. Capillary forces are associated with a network that connects the centroids of grains where a meniscus exists. The attraction force can be computed based on analytical theories of capillary force between spherical bodies [Orr et al., 1975; Lian et al., 1993; Willett et al., 2000]. Depending on the degree of accuracy required, approximations of increasing complexity can be made. The forces computed will then be used as loads on a grain-by-grain basis in the DEM code PFC3D.

The key novelty is the accurate consideration, for the first time, of multiphase systems in grain-scale mechanics. The success of this approach relies on the accurate prediction of the gas–water

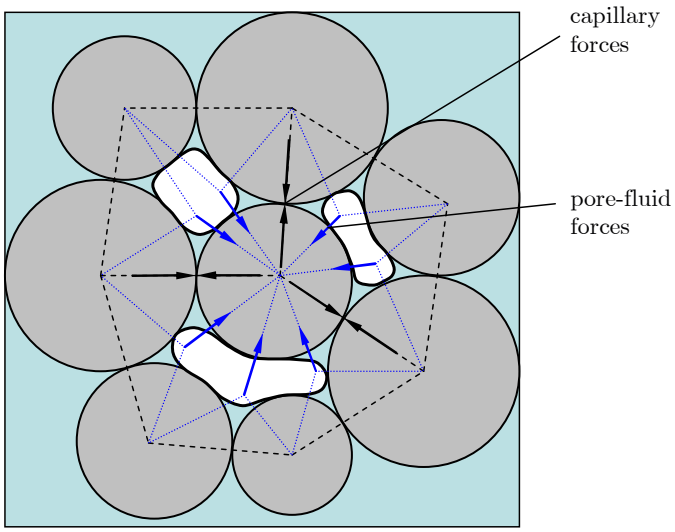

Figure 17: Schematic diagram of the networks of grain–pore body fluid forces (in blue) and grain–grain capillary forces (in black) in a DEM model. These force networks are required to model grain-scale mechanics in the presence of multiphase fluid displacements, and must be supplemented to the grain–grain network of contact forces shown in Figure 16.

interface offered by the level set method. From a fundamental point of view, this coupled model will lead to a *mechanistic* definition of effective stress in two-fluid granular systems (as opposed to a thermodynamic definition [Borja, 2006]).

Coupled capillarity and hydrate formation models. Here we evaluate the grain-scale consequences of forming hydrate at gas-water interfaces after methane has drained into sediment. We consider two limiting cases: constant gas phase pressure P_g, and P_g decreasing as hydrate grows. The first case corresponds to an infinite supply of methane. The second case corresponds to a disconnected volume of methane.

For both cases we establish the drainage endpoint at the initial value of P_g using the methods described above. Because the gas-water interface geometry is also known at the grain scale, we then compute the volume of hydrate formed as function of hydrate thickness. We also note the characteristic length scale of volumes of pore water within the drained volume. From the already computed water saturation, we compute the average salinity increase as function of hydrate volume. The characteristic size of volumes of water provides a time scale at which this average salinity is reached. We can then determine when the limit of hydrate stability is reached due to salinity increase. At this point we can compute the volume of free gas remaining in drained zone.

In the case of a finite volume of gas, we also compute the reduction in P_g as a function of hydrate volume. We will consider the conditions for breaking the hydrate layer in a pore throat. Because the detailed interface geometry is available, we will also evaluate the conditions for dislodging a hydrate layer from the gas-water-solid contact lines in a throat. We will determine when growing individual skins of hydrate in pore throats join to become a single surface, which will have significantly more resistance to being dislodged. In the event that hydrate ruptures or is dislodged, we will compute the subsequent imbibition events and repeat the evaluation of hydrate formation.

Coupled mechanics and hydrate formation models. We will develop a strategy for integrating capillary-driven displacement subject to hydrate formation (as explained above) with grain-scale mechanics. Precipitation of crystalline hydrate at the gas–water interface and subsequent thickening of the hydrate shell will affect the strength of the packing. This effect can be modeled explicitly in a DEM code by assigning cement strengths to grain contacts that exhibit hydrate precipitation [Potyondy and Cundall, 2004]. Given a precise distribution of hydrate in the pore space, we will compute the gas pressure required to either re-open a previous fracture that has been cemented or to open a new fracture. In either case, we expect that the interplay between capillary invasion, hydrate precipitation, and mechanical strength will lead to a complex distribution of methane in the pore space.

Methane transport and hydrate formation at the bed scale: a threshold/leakage model. We will integrate the process models developed above into a threshold/leakage model. This model will describe methane movement vertically and laterally within the HSZ from a postulated source below the HSZ. The "threshold" refers to the criteria for vertical gas phase movement (fracture initiation or drainage) and for lateral gas movement from a fracture into a sediment bed. These criteria will be determined in the models discussed above. The "leakage" refers to the movement of methane laterally into sediment beds satisfying the threshold criteria. Should vertical movement continue all the way to the sea floor, the leakage term will include the flux of methane into the ocean.

The thresholds in this model depend on capillary pressure $P_c = P_g - P_w$, as depicted in (**Figure 8**), and so P_c will be the primary variable. The dynamics of this model derive from the following observations:

- buoyancy causes P_c at the top of the rising gas to increase as it rises, as long as it remains connected to the source below the HSZ
- vertical variation in sediment properties makes the evaluation of thresholds nontrivial, even though P_c increases with elevation
- lateral movement of methane into a sediment bed will be driven by capillary forces, establishing a water saturation S_w that depends only on P_c and hence upon elevation; S_w may therefore vary within a bed that is invaded. The rate at which methane enters the bed will depend on the gas relative permeability at the relevant values of S_w.
- if the methane source below the HSZ is finite and is being charged slowly, then leakage of methane into sediment beds will result in water rising into the bottom of the methane source. This will *reduce* P_c uniformly in the column of rising methane, causing hysteresis and requiring re-evaluation of thresholds.

Mathematically, we cast this as a quasi-1D mass balance in integral form, with elevation z being the one dimension. The initial condition is a methane source of thickness h bounded above by the HSZ and below by water-saturated sediment. P_c is zero at the methane-water contact and increases linearly with elevation. Movement of methane begins at a threshold P_c that depends on

the properties of the sediment overlying the source. The P_c profile through the HSZ is constructed and the threshold criteria are evaluated along z. This results in a set of intervals $[z_i,z_{i+1}]$ along which leakage occurs. Leakage rates are postulated as $q(z) = \eta(z)P_c(z)$ where η is a mass transfer coefficient that includes absolute permeability of the bed, relative permeability at the prevailing saturate S_w and viscosity. Only the relative magnitudes of η between and within beds matter. If methane rises all the way to the seafloor, the flux into the ocean will be proportional to the hydraulic conductance of the flow path.

The cumulative mass that leaks through the intervals $[z_i,z_{i+1}]$ is equal to the mass no longer in the methane source. The gas-water contact must rise to fill the evacuated volume within the source region. The corresponding decrease in P_c is readily determined.

To account for the distribution of hydrate in this model, we first examine the behavior for the following limiting case assumptions:

- Assume upward movement of methane is only through sediment not yet containing hydrate.
- Assume hydrate forms at gas-water interface.
- Assume hydrate forms only when (local) movement is halted, either by resistance to further movement or by loss of pressure in gas phase.

The last assumption is equivalent to assuming time scale for interface movement is short compared to timescale for heat of crystallization to be dissipated.

The threshold/leakage model determines the vertical saturation profile $S_w(z)$ that will prevail for a given distribution of sediment properties. We remark that the initial thickness of the postulated methane source can be deduced from the P_c required to initiate a fracture or start drainage. The relative volumes of methane that enter multiple beds are readily determined. The ultimate distribution of methane between free gas and hydrate at any given elevation within an invaded bed depends on the S_w reached at that elevation and upon the extent of hydrate rupture that occurred if and when P_c began to decrease. These dependencies will have been worked out in the finer scale modeling.

The threshold/leakage model is deliberately simple to permit testing the implications of the grain-scale models.

2.2.3 Risks and Limitations

Like any modeling study, the proposed work runs the risk of failing to include important mechanisms or processes in the model. Unlike many modeling studies, the approach here is entirely mechanistic. This enables truly *a priori* predictions, which in turn permit rigorous testing of the models. Suppose, for example, that predicted behavior is not consistent with field observations. It is not possible to adjust parameters in the model in order to improve the fit, for the simple reason that all parameters can be independently determined. Instead we would conclude that (at least) one premise of the model, e.g. hydrates are formed only at the gas/water interface, is not valid. The approach thereby avoids the risk of getting the right answer for the wrong reason. It also provides some guidance as to what phenomena or processes should be added to the model if it fails to explain observations.

The other principal risk is sacrificing complexity in the physics for the sake of making the problem tractable. Our experience with the methods to be used will help reduce this risk. For example, thermal effects are currently not directly considered in the project. However, we may decide to incorporate them as we identify they are essential. Indeed, we plan to extend the work proposed here in the following directions:

1. Thermal effects (both at the microscale and the bed-scale).
2. Seismic attenuation at the microscale.
3. Micromodel and tank experiments.

3 FUTURE

3.1 Barriers Research will Overcome

We summarize the barriers that this research will overcome in the following set of **scientific objectives**:

1. Understand the mechanisms that control the presence, migration, entrapment and destabilization of methane hydrates in ocean sediments, including:
   - Drainage of methane gas and subsequent hydrate formation at the pore scale.
   - Modeling of methane trapping in the pore space.
   - Coupling with sediment mechanics: activation of faults or opening of fractures that serve as conduits for focused methane gas flow.
2. Explain the co-existence of methane gas and methane hydrate within the HSZ in hydrodynamically active environments, based on the above results and:
   - Increased salinity of pore water upon hydrate formation.
   - Availability of gas–water interface.
3. Describe the dynamics within the HSZ, by means of numerical models that capture:
   - Upwards migration of gas through HSZ (capillary and fracture invasion).
   - Entrapment of gas by capillary imbibition and hydrate formation.
   - Competition between vertical flow (through beds) and lateral flow (along beds).

Our experience in grain-scale capillary displacement and solid mechanics leads us to make the following conjecture: the intricate multiphase flow–mechanics behavior will lead to a characteristic distribution of hydrate that includes co-existence with gas, both laterally and vertically within a sediment column. This project would bring together the computational tools needed to quantify these concepts.

We want to emphasize that our bed-scale modeling will benefit in a direct and essential way from the pore-scale modeling effort. Moreover, this approach will complement that of other investigations, including projects funded under the DOE/NETL Methane Hydrates program.

3.2 Potential Impact on the Understanding of Hydrate's Role in the Natural Environment

The goal of this project is to understand quantitatively the manner in which methane is transported within the HSZ. The research will seek (in)validation of the following hypothesis: the coupling between geomechanics, the dynamics of gas/water interfaces, and phase behavior of the gas/brine/hydrate system make co-existence of free gas and hydrate inevitable in the HSZ.

If borne out, our hypothesis would provide a mechanistic basis for several observations of co-existing gas and hydrate in the HSZ. The model have implications for interpretation of seismic and borehole log data and thus for estimates of carbon held in the HSZ. It would explain the apparent lateral and vertical variability in hydrate saturation, e.g. preferential occurrence in coarse grained material above and below a fine grained layer. The model would be a step toward explaining active and passive hydrate accumulations with a single set of mechanisms.

3.3 Deliverables

Periodic, topical, financial, and final reports shall be submitted as required in accordance with the Federal Assistance Reporting Checklist and in accordance with the requirements of the solicitation under which this work was proposed. Additional deliverables for this study are described along with each Task and Subtask of the Statement of Project Objectives.

We will prepare detailed briefings for presentation to the Project Officer at the Project Officer's facility located in Pittsburgh, PA or Morgantown, WV. Briefings shall be given by the Recipient to explain the plans, progress, and results of the technical effort on an annual basis.

We will pursue technology-transfer activities, including peer-reviewed publications, paper and/or poster presentations at professional meetings, and technology transfer workshops. The PIs and Dr. Prodanovic have also participated in major code development projects that resulted in publicly available software. The bed-scale model and the level set methods for capillarity developed in this work will be made available.

REFERENCES

C. H. Arns, A. Sakellariou, T. J. Senden, A. P. Sheppard, R. M. Sok, W. V. Pinczewski, and M. A. Knackstedt. Petrophysical properties derived from X-ray CT images. *APPEA J.*, 43:577–586, 2003.

M. M. Backus, P. E. Murray, B. A. Hardage, and R. J. Graebner. High-resolution multicomponent imaging of deepwater gas–hydrate systems. *The Leading Edge*, 25:578–598, 2006.

M. A. Biot. General theory of three-dimensional consolidation. *J. Appl. Phys.*, 12:155–164, 1941.

M. Blunt and M. Hilpert. Editorial. *Adv. Water Resour.*, 24:231–232, 2001.

R. I. Borja. On the mechanical energy and effective stress in saturated and unsaturated porous continua. *Int. J. Solids Structures*, 43(6):1764–1786, 2006.

B. P. Boudreau, C. Algar, B. D. Johnson, I. Croudace, A. Reed, Y. Furukawa, K. M. Dorgan, P. A. Jumars, and A. S. Grader. Bubble growth and rise in soft sediments. *Geology*, 33(6):517–520, doi:10.1130/G21259.1, 2005.

J. Bradley. Fluid and electrical formation conductivity factors calculated for a spherical-grain onion-skin model. *Log Analyst*, pages 24–32, Jan/Feb 1980.

M. S. Bruno. Micromechanics of stress-induced permeability anisotropy and damage in sedimentary rocks. *Mech. Mater.*, 18:31–48, 1994.

M. S. Bruno and R. B. Nelson. Microstructural analysis of the inelastic behavior of sedimentary rock. *Mech. Mater.*, 12(2):95–118, 1991.

S. Bryant, C. Cade, and D. Mellor. Physically representative network models of transport in porous media. *AIChE J.*, 39:387–396, 1993.

S. Bryant and A. Johnson. Bulk and film contributions to fluid/fluid interfacial area in granular media. *Chem. Eng. Comm.*, 191, 2004.

S. Bryant, G. Mason, and D. Mellor. Quantification of spatial correlation in porous media and its effect on mercury porosimetry. *J. Colloid Interface Sci.*, 177:88–100, 1996.

G. E. Claypool et al., editors. *The Gulf of Mexico Gas Hydrate Joint Industry Project*, Final Cruise Report, 2006. http://www.netl.doe.gov/technologies/oil-gas/publications/Hydrates/reports/GOMJIPCruise05.pdf.

M. B. Clennell, M. Hovland, J. S. Booth, P. Henry, and W. J. Winters. Formation of natural gas hydrates in marine sediments 1. Conceptual model of gas hydrate growth conditioned by host sediment properties. *J. Geophys. Res.*, 104(B10):22985–23003, 1999.

T. S. Collett. Energy resource potential of natural gas hydrates. *AAPG Bull.*, 86(11):1971–1992, 2002.

B. K. Cook, D. R. Noble, and J. R. Williams. A direct simulation method for particle-fluid systems. *Eng. Comput.*, 21(2–4):151–168, 2004.

P. A. Cundall and O. D. L. Strack. Discrete numerical model for granular assemblies. *Geotechnique*, 29: 47–65, 1979.

M. K. Davie and B. A. Buffett. A numerical model for the formation of gas hydrate below the seafloor. *J. Geophys. Res.*, 106(B1):497–514, 2001.

M. K. Davie and B. A. Buffett. Sources of methane for marine gas hydrate: inferences from a comparison of observations and numerical models. *Earth Planet. Sci. Lett.*, 206:51–63, 2003.

G. R. Dickens. The blast in the past. *Nature*, 401:752–755, 1999.

G. R. Dickens. Rethinking the global carbon cycle with a large, dynamic and microbially mediated gas hydrate capacitor. *Earth Planet. Sci. Lett.*, 213:169–183, 2003.

G. R. Dickens, C. K. Paull, and P. Wallace. Direct measurement of in situ methane quantities in a large gas-hydrate reservoir. *Nature*, 385:426–428, 1997.

W. B. Durham, L. A. Stern, S. H. Kirby, and S. Circone. Rheological comparisons and structural imaging of sI and sII end-member gas hydrates and hydrate/sediment aggregates. In *Proc. Fifth Intl. Conf. Gas Hydrates*, Trondheim, Norway, 2005.

J. Dvorkin, M. B. Helgerud, W. F. Waite, S. H. Kirby, and A. Nur. Introduction to physical properties and elasticity models. In M. D. Max, editor, *Natural Gas Hydrate in Oceanic and Permafrost Environments*, pages 245–260, Dordrecht, The Netherlands, 2000. Kluwer.

T. Ebinuma, Y. Kamata, and H. Minagawa. Mechanical properties of sandy sediment containing methane hydrate. In *Proc. Fifth Intl. Conf. Gas Hydrates*, Trondheim, Norway, 2005.

C. Ecker, J. Dvorkin, and A. Nur. Sediments with gas hydrates: Internal structure from seismic AVO. *Geophysics*, 63(5):1659–1669, 1998.

I. Fatt. The network model of porous media I. Capillary pressure characteristics. *Trans. AIME*, 207:144–159, 1956.

J. L. Finney. Random packings and the structure of simple liquids. I. The geometry of random close packing. *Proc. Roy. Soc. Lond. A*, 319:479–493, 1970.

P. B. Flemings, X. Liu, and W. J. Winters. Critical pressure and multiphase flow in Blake Ridge gas hydrates. *Geology*, 31(12):1057–1060, 2003.

J. Fredrich and W. B. Lindquist. Statistical characterization of the three-dimensional microgeometry of porous media and correlation with macroscopic transport properties. *Int. J. Rock Mech. Min. Sci.*, 34: 3–4, 1997.

G. Genov, W. F. Kuhs, D. K. Staykova, E. Goreshnik, and A. N. Salamatin. Experimental studies on the formation of porous gas hydrates. *Am. Mineral.*, 89:1228–1239, 2004.

G. D. Ginsburg and V. A. Soloviev. Methane migration within the submarine gas-hydrate stability zone under deep-water conditions. *Mar. Geol.*, 137:49–57, 1997.

M. Gladkikh and S. Bryant. Prediction of interfacial areas during imbibition in simple porous media. *Adv. Water Resour.*, 26:609–622, 2003.

M. Gladkikh and S. Bryant. Prediction of imbibition in unconsolidated granular materials. *J. Colloid Interface Sci.*, 288:526–539, 2005.

A. R. Gorman, W. S. Holbrook, M. J. Hornbach, K. L. Hackwith, D. Lizarralde, and I. Pecher. Migration of methane gas through the hydrate stability zone in a low-flux hydrate province. *Geology*, 30(4):327–330, 2002.

L. Graton and H. Fraser. Systematic packing of spheres with particular relation to porosity and permeability. *J. Geol.*, 43:785–909, 1935.

G. Guerin, D. Goldberg, and A. Meltser. Characterization of in situ elastic properties of gas hydrate-bearing sediments on the Blake Ridge. *J. Geophys. Res.*, 104(B8):17781–17795, 1999.

F. Hackett and J. Strettan. The capillary pull of an ideal soil. *J. Agr. Sci*, 18:671–681, 1928.

W. B. Haines. Studies in the physical properties of soils. II. A note on the cohesion developed by capillary forces in an ideal soil. *J. Agr. Sci.*, 15:529–535, 1925.

W. B. Haines. Studies in the physical properties of soils. IV. A further contribution to the theory of capillary phenomena in soil. *J. Agr. Sci.*, 17:264–290, 1927.

K. U. Heeschen, A. M. Trehu, R. W. Collier, E. Suess, and G. Rehder. Distribution and height of methane bubble plumes on the Cascadia Margin characterized by acoustic imaging. *Geophys. Res. Lett.*, 30(12): Art. No. 1643, doi:10.1029/2003GL016974, 2003.

M. B. Helgerud, J. Dvorkin, and A. Nur. Elastic-wave velocity in marine sediments with gas hydrates: Effective medium modeling. *Geophys. Res. Lett.*, 26(13):2021–2024, 1999.

P. Henry, M. Thomas, and M. B. Clennell. Formation of natural gas hydrates in marine sediments 2. Thermodynamic calculations of stability conditions in porous sediments. *J. Geophys. Res.*, 104(B10): 23005–23022, 1999.

J. W. D. Hobro, T. A. Minshull, S. C. Singh, and S. Chand. A three-dimensional seismic tomographic study of the gas hydrate stability zone, offshore Vancouver Island. *J. Geophys. Res.*, 110:B09102, doi:10.1029/2004JB003477, 2005.

W. S. Holbrook, H. Hoskins, W. T. Wood, R. A. Stephen, and D. Lizarralde. Methane hydrate and free gas on the Blake Ridge from vertical seismic profiling. *Science*, 273:1840–1842, September 27, 1996.

G. D. Holder, V. A. Kamath, and S. P. Godbole. The potential of natural gas hydrates as an energy resource. *Ann. Rev. Energy*, 9:427–445, 1984.

S. Holditch, T. Patzek, G. Moridis, and R. Plumb. Geomechanical performance of hydrate-bearing sediments in offshore environments. Semi-Annual Report DOE Award Number DE-FC26-05NT42664, Department of Energy, July 2006.

M. J. Hornbach, D. M. Saffer, and W. S. Holbrook. Critically pressured free-gas reservoirs below gas-hydrate provinces. *Nature*, 427(6970):142–144, 2004.

ITASCA. *PFC3D, v3.1 – Theory and Background.* Itasca Consulting Group, Inc., Minneapolis, MN, 2005.

G. Jin. *Physics-Based Modeling of Sedimentary Rock Formation and Prediction of Transport Properties.* PhD Dissertation, University of California at Berkeley, Spring 2006.

G. Jin, T. W. Patzek, and D. B. Silin. Physics based reconstruction of sedimentary rocks. In *SPE Western Regional/AAPG Pacific Section Joint Meeting*, Long Beach, CA, May 19–24 2003. (SPE 83587).

B. D. Johnson, B. P. Boudreau, B. S. Gardiner, and R. Maass. Mechanical response of sediments to bubble growth. *Mar. Geol.*, 187:347–363, 2002.

R. Juanes, E. J. Spiteri, F. M. Orr, Jr., and M. J. Blunt. Impact of relative permeability hysteresis on geological CO_2 storage. *Water Resour. Res.*, 42:doi:10.1029/2005WR004806, 2006.

A. G. Judd, M. Hovland, L. I. Dimitrov, S. Garcia Gil, and V. Jukes. The geological methane budget at Continental Margins and its influence on climate change. *Geofluids*, 2:109–126, 2002.

R. L. Kleinberg, C. Flaum, D. D. Griffin, P. G. Brewer, G. E. Malby, E. T. Pelzer, and J. P. Yesinowski. Deep sea NMR: Methane hydrate growth habit in porous media and its relationship to hydraulic permeability, deposit accumulation, and submarine slope stability. *J. Geophys. Res.*, 108(B10):2508, doi:10.1029/2003JB002389, 2003.

A. Kumar, R. Ozah, M. Noh, G. A. Pope, S. Bryant, K. Sepehrnoori, and L. W. Lake. Reservoir simulation of CO_2 storage in deep saline aquifers. *Soc. Pet. Eng. J.*, 10(3):336–348, September 2005.

K. A. Kvenvolden. Methane hydrate – a major reservoir of carbon in the shallow geosphere? *Chem. Geol.*, 71:41–51, 1988.

K. A. Kvenvolden, G. D. Ginsburg, and V. A. Soloviev. Worldwide distribution of subaquatic gas hydrates. *Geo-Mar. Lett.*, 13:32–40, 1993.

J.-Y. Lee, T. S. Yun, J. C. Santamarina, and C. Ruppel. Observations related to tetrahydrofuran and methane hydrate for laboratory studies of hydrate-bearing sediments. *Geochem. Geophys. Geosyst.*, 2006. (Submitted).

G. Lian, C. Thornton, and M. J. Adams. A theoretical study of the liquid bridge forces between two rigid spherical bodies. *J. Colloid Interface Sci.*, 161:138–147, 1993.

W. B. Lindquist, A. Venkatarangan, J. Dunsmuir, and T.-F. Wong. Pore and throat size distributions measured from synchrotron X-ray tomographic images of Fontainebleau sandstones. *J. Geophys. Res.*, 105B:21508–21528, 2000.

X. Liu and P. B. Flemmings. Passing gas through the hydrate stability zone at southern Hydrate Ridge, offshore Oregon. *Earth Planet. Sci. Lett.*, 241:211–216, 2006.

G. Mason. Desaturation of porous media. I. Unconsolidated materials. *J. Colloid Interface Sci.*, 41:208–227, 1972.

G. Mason and D. Mellor. Simulation of drainage and imbibition in a random packing of equal spheres. *J. Colloid Interface Sci.*, 176:214–225, 1995.

A. Masui, H. Haneda, Y. Ogata, and K. Aoki. The effect of saturation degree of methane hydrate on the shear strength of synthetic methane hydrate sediment. In *Proc. Fifth Intl. Conf. Gas Hydrates*, Trondheim, Norway, 2005.

J. Melrose. Wettability as related to capillary action in porous media. *Soc. Pet. Eng. J.*, September:259–271, 1965.

A. V. Milkov. Global estimates of hydrate-bound gas in marine sediments: how much is really out there? *Earth-Sci. Rev.*, 66:183–197, 2004.

A. V. Milkov, G. E. Claypool, Y.-J. Lee, G. R. Dickens, W. Xu, W. S. Borowski, and Leg 204 Science Party. In situ methane concentrations at Hydrate Ridge offshore Oregon: new constraints on the global gas inventory from an active margin. *Geology*, 30:833–836, 2003.

A. V. Milkov, G. E. Claypool, Y.-J. Lee, M. E. Torres, W. S. Borowski, H. Tolmaru, R. Sassen, P. Long, and Leg 204 Scientific Party. Ethane enrichment, propane depletion, and other compositional variations in subsurface gases: A new indicator of gas hydrate occurrence in marine sediments. *Org. Geochem.*, 35: 1067–1080, 2004a.

A. V. Milkov, G. R. Dickens, G. E. Claypool, Y.-J. Lee, W. S. Borowski, M. E. Torres, W. Xu, H. Tomaru, A. M. Trehu, and P. Schultheiss. Co-existence of gas hydrate, free gas, and brine within the regional gas hydrate stability zone at Hydrate Ridge (Oregon margin): evidence from prolongued degassing of a pressurized core. *Earth Planet. Sci. Lett.*, 222:829–843, 2004b.

A. V. Milkov and W. Xu. Comment on "Gas hydrate growth, methane transport, and chloride enrichment at the southern summit of Hydrate Ridge, Cascadia margin off Oregon" by Torres et al. [Earth Planet. Sci. Lett. 226:225–241 (2004)]. *Earth Planet. Sci. Lett.*, 239:162–167, 2005.

G. J. Moridis. Numerical studies of gas production from methane hydrates. *Soc. Pet. Eng. J.*, pages 359–370, December 2003.

G. J. Moridis, T. S. Collett, S. R. Dallimore, T. Inoue, and T. Mroz. Analysis and interpretation of the thermal test of gas hydrate dissociation in the JAPEX/JNOC/GSC et al. Mallik 5L-38 gas hydrate production research well. In S. R. Dallimore and T. S. Collett, editors, *Scientific Results from the Mallik 2002 Gas Hydrate Production Research Well Program, Mackenzie Delta, Northwest Territories, Canada.* Geological Survey of Canada, Bulletin 585, 2005.

G. J. Moridis, T. S. Collett, S. R. Dallimore, T. Satoh, S. Hancock, and B. Weatherill. Numerical studies of gas production from several CH_4 hydrate zones at the Mallik site, Mackenzie Delta, Canada. *J. Pet. Sci. Eng.*, 43:219–238, 2004.

N. Morrow and C. Graves. On the properties of equal sphere packings and their use as ideal soils. *Soil Sci.*, 108:102–107, 1970.

Y. Muguruma, T. Tanaka, and Y. Tsuji. Numerical simulation of particulate flow with liquid bridge between particles (simulation of centrifugal tumbling granulator). *Powder Technol.*, 109:49–57, 2000.

J. Nimblett and C. Ruppel. Permeability evolution during the formation of gas hydrates in marine sediments. *J. Geophys. Res.*, 108(B9):2420, doi:10.1029/2001JB001650, 2003.

F. M. Orr, L. E. Scriven, and A. P. Rivas. Pendular rings between solids: meniscus properties and capillary force. *J. Fluid Mech.*, 67:723–742, 1975.

S. Osher and R. Feldkiw. *Level Set Methods and Dynamic Implicit Surfaces.* Springer-Verlag, 2002.

S. Osher and J.A. Sethian. Fronts propagating with curvature dependent speed: algorithms based on Hamilton-Jacobi formulation. *J. Comp. Phys.*, 79:12–49, 1988.

C. K. Paull, P. G. Brewer, W. Ussler, E. T. Peltzer, G. Rehder, and D. Clague. An experiment demonstrating that marine slumping is a mechanism to transfer methane from seafloor gas-hydrate deposits into the upper ocean and atmosphere. *Geo-Mar. Lett.*, 22:198–203, 2003.

C. K. Paull, W. J. Buelow, W. Ussler, and W. S. Borowski. Increased continental-margin slumping frequency during sea-level lowstands above gas hydrate-bearing sediments. *Geology*, 24:143–146, 1996.

C. K. Paull, R. Matsumoto, P. J. Wallace, and W. P. Dillon, editors. *Gas Hydrates Sampling on the Blake Ridge and Carolina Rise*, volume 164 of *Proc. ODP, Sci. Results*, College Station, TX, 2000. Ocean Drilling Program.

S. Pirson. Factors which affect true formation resistivity. *Oil Gas J.*, 1:76–81, 1947.

D. O. Potyondy and P. A. Cundall. A bonded-particle model for rock. *Int. J. Rock Mech. Min. Sci.*, 41: 1329–1364, 2004.

M. Prodanovic and S. Bryant. Investigating pore scale configurations of two immiscible fluids via the level set method. In *Computational Methods in Water Resources XVI*, 2006a. To appear.

M. Prodanovic and S. Bryant. Critical curvatures for drainage and imbibition via level set methods. *J. Colloid Interface Sci.*, 2006b. In preparation.

H. Rajaram, L. A. Ferrand, and M. A. Celia. Prediction of relative permeabilities for unconsolidated soils using pore-scale network models. *Water Resour. Res.*, 33:43–52, 1997.

P. C. Reeves and M. A. Celia. A functional relationship between capillary pressure, saturation, and interfacial areas as revealed by a pore-scale network model. *Water Resour. Res.*, 32:2345–2358, 1996.

A. W. Rempel and B. A. Buffett. Formation and accumulation of gas hydrate in porous media. *J. Geophys. Res.*, 102(B4):10151–10164, 1997.

M. Riedel, T. S. Collett, M. J. Malone, and the Expedition 311 Scientists, editors. *Cascadia Margin Gas Hydrates*, volume 311 of *Proc. IODP, Expedition Reports*, College Station, TX, 2006. Integrated Ocean Drilling Program.

H. H. Roberts, B. A. Hardage, W. W. Shedd, and J. Hunt, Jr. Seafloor reflectivity – An important seismic property for interpreting fluid/gas expulsion geology and the presence of gas hydrates. *The Leading Edge*, 25:620–628, 2006.

J. N. Roberts and L. M. Schwartz. Grain consolidation and electrical conductivity in porous media. *Phys. Rev. B*, 31:5990–5997, 1985.

C. Ruppel. Anomalously cold temperatures observed at the base of the gas hydrate stability zone. *Geology*, 25:699–702, 2000.

C. Ruppel. Tapping methane hydrates for unconventional natural gas. *Elements*, 2006. (In Review).

C. Ruppel, G. R. Dickens, D. G. Castellini, W. Gilhooly, and D. Lizarralde. Heat and salt inhibition of gas hydrate formation in the northern Gulf of Mexico. *Geophys. Res. Lett.*, 32:L04605, doi:10.1029/2004GL021909, 2005.

J. A. Sethian. *Level Set Methods and Fast Marching Methods*. Cambridge University Press, 1999.

Y. Shimizu. Fluid coupling in PFC2D and PFC3D. In Y. Shimizu, R. D. Hart, and P. Cundall, editors, *Numerical Modeling in Micromechanics Via Particle Methods. Proc. of the 2nd International PFC Symposium, Kyoto, Japan*, pages 281–287, Balkema, Leiden, October 2004.

G. C. Sills, S. J. Wheeler, S. D. Thomas, and T. N. Gardner. Behavior of offshore soils containing gas bubbles. *Geotechnique*, 41(2):227–241, 1991.

C. Slichter. Theoretical investigations of the motions of groundwaters. Technical Report 306, U.S. Geol. Surv. Ann. Rept., 1899.

E. D. Sloan. *Clathrate Hydrates of Natural Gases*. Marcel Deker, New York, second edition, 1998.

E. D. Sloan. Fundamental principles and applications of natural gas hydrates. *Nature*, 426:353–359, November 23, 2003.

V. A. Soloviev and G. D. Ginsburg. Water segregation in the course of gas hydrate formation and accumulation in submarine gas-seepage fields. *Mar. Geol.*, 137:59–68, 1997.

R. D. Stoll, J. Ewing, and G. M. Bryan. Anomalous wave velocities in sediments containing gas hydrates. *J. Geophys. Res.*, 76:2090–2094, 1971.

E. Suess, M. E. Torres, G. Bohrmann, R. W. Collier, J. Greiner, P. Linke, G. Rehder, A. Trehu, K. Wallman, G. Winckler, and E. Zuleger. Gas hydrate destabilization: enhanced dewatering, benthic material turnover and large methane plumes at the Cascadia convergent margin. *Earth Planet. Sci. Lett.*, 170:1–15, 1999.

C. Thane. Random sphere packings: A theoretical study of the liquid bridge forces between two rigid spherical bodies. MS Thesis, The University of Texas at Austin, 2006.

U. Tinivella and F. Accaino. Compressional velocity structure and Poisson's ratio in marine sediments with gas hydrate and free gas by inversion of reflected and refracted seismic data (South Shetland Islands, Antarctica. *Mar. Geol.*, 164:13–27, 2000.

B. Tohidi, R. Anderson, M. B. Clennell, R. W. Burgass, and A. B. Biderkab. Visual observation of gas-hydrate formation and dissociation in synthetic porous media by means of glass micromodels. *Geology*, 29(9):867–870, 2001.

S. Torquato. *Random Heterogeneous Materials: Microstructure and Macroscopic Properties*. Springer-Verlag, New York, 2002.

M. E. Torres, K. Wallman, A. M. Trehu, G. Bohrmann, W. S. Borowski, and H. Tomaru. Gas hydrate growth, methane transport, and chloride enrichment at the southern summit of Hydrate Ridge, Cascadia margin off Oregon. *Earth Planet. Sci. Lett.*, 226:225–241, 2004.

M. E. Torres, K. Wallman, A. M. Trehu, G. Bohrmann, W. S. Borowski, and H. Tomaru. Reply to comment on: "Gas hydrate growth, methane transport, and chloride enrichment at the southern summit of Hydrate Ridge, Cascadia margin off Oregon". *Earth Planet. Sci. Lett.*, 239:168–175, 2005.

A. M. Trehu, G. Bohrmann, M. E. Torres, and F. S. Colwell, editors. *Drilling Gas Hydrates on Hydrate Ridge, Cascadia Continental Margin*, volume 204 of *Proc. ODP, Sci. Results*, College Station, TX, 2006a. Ocean Drilling Program. doi:10.2973/odp.proc.sr.204.2006.

A. M. Trehu, P. B. Flemings, N. L. Bangs, J. Chevalier, E. Gracia, J. E. Johnson, C.-S. Liu, X. Liu, M. Riedel, and M. E. Torres. Feeding methane vents and gas hydrate deposits at south Hydrate Ridge. *Geophys. Res. Lett.*, 31:L23310, doi:10.1029/2004GL021286, 2004a.

A. M. Trehu, P. E. Long, M. E. Torres, G. Bohrmann, F. R. Rack, T. S. Collett, D. S. Goldberg, A. V. Milkov, M. Riedel, P. Schultheiss, N. L. Bangs, S. R. Barr, W. S. Borowski, G. E. Claypool, M. E. Delwiche, G. R. Dickens, E. Gracia, G. Guerin, M. Holland, J. E. Johnson, Y. J. Lee, C. S. Liu, X. Su, B. Teichert, H. Tomaru, M. Vanneste, M. Watanabe, and J. L. Weinberger. Three-dimensional distribution of gas hydrate beneath southern Hydrate Ridge: constraints from ODP Leg 204. *Earth Planet. Sci. Lett.*, 222: 845–862, 2004b.

A. M. Trehu, C. Ruppel, M. Holland, G. R. Dickens, M. E. Torres, T. S. Collett, D. Goldberg, R. Riedel, and P. Schultheiss. Gas hydrates in marine sediments: lessons from scientific drilling. *Oceanography*, 2006b. (In Press).

M. D. Tryon, K. M. Brown, and M. E. Torres. Fluid and chemical flux in and out of sediments hosting methane hydrate deposits on Hydrate Ridge, OR, II: Hydrological processes. *Earth Planet. Sci. Lett.*, 201:541–557, 2002.

W. F. Waite, W. J. Winters, and D. H. Mason. Methane hydrate formation in partially water-saturated Ottawa sand. *Am. Mineral.*, 89:1202–1207, 2004.

J. L. Weinberger and K. M. Brown. Fracture networks and hydrate distribution at Hydrate Ridge, Oregon. *Earth Planet. Sci. Lett.*, 245:123–136, 2006.

J. L. Weinberger, K. M. Brown, and P. E. Long. Painting a picture of gas hydrate distribution with thermal images. *Geophys. Res. Lett.*, 32:L04609, doi:10.1029/2004GL021437, 2005.

K. A. Weitemeyer, S. C. Constable, K. W. Key, and J. P. Behrens. First results from a marine controlled-source electromagnetic survey to detect gas hydrates offshore Oregon. *Geophys. Res. Lett.*, 33:L03304, doi:10.1029/2005GL024896, 2005.

S. J. Wheeler. A conceptual model for soils containing large gas bubbles. *Geotechnique*, 38:389–397, 1988.

D. Wilkinson and J. Willemsen. Invasion percolation: a new form of percolation theory. *J. Phys. A*, 16: 3365–3376, 1983.

C. D. Willett, M. J. Adams, S. A. Johnson, and J. P. K. Seville. Capillary bridges between two spherical bodies. *Langmuir*, 16:9396–9405, 2000.

E. C. Willoughby, K. Schwalenberg, R. N. Edwards, G. D. Spence, and R. D. Hyndman. Assessment of marine gas hydrate deposits: a comparative study of seismic, electromagnetic and seafloor compliance methods. In *Proc. Fifth Intl. Conf. Gas Hydrates*, Trondheim, Norway, 2005.

C. S. Willson, R. W. Stacey, K. Ham, and K. E. Thompson. Investigating the correlation between residual nonwetting phase liquids and pore-scale geometry and topology using synchrotron X-ray tomography. *SPIE 5535 Developments in X-ray Tomography*, 5535:101–111, 2004.

W. J. Winters, I. A. Pecher, W. F. Waite, and D. H. Mason. Physical properties and rock physics models of sediment containing natural and laboratory-formed methane hydrate. *Am. Mineral.*, 89:1221–1227, 2004.

W. Xu and C. Ruppel. Predicting the occurrence, distribution, and evolution of methane gas hydrate in porous marine sediments. *J. Geophys. Res.*, 104(B3):5081–5095, 1999.

R. Y. Yang, R. P. Zou, and A. B. Yu. Numerical study of the packing of wet coarse uniform spheres. *AIChE J.*, 49(7):1656–1666, 2003.

T. S. Yun, F. M. Francisca, J. C. Santamarina, and C. Ruppel. Compressional and shear wave velocities in uncemented sediment containing gas hydrate. *Geophys. Res. Lett.*, 32:L10609, doi:10.1029/2005GL022607, 2005.

T. S. Yun, J. C. Santamarina, and C. Ruppel. Mechanical properties of sand, silt and clay containing synthetic hydrate. *J. Geophys. Res.*, 2006. (In Review).

O. Y. Zatsepina and B. A. Buffett. Nucleation of gas hydrate in marine environments. *Geophys. Res. Lett.*, 30(9):1451, doi:10.1029/2002GL016802, 2003.